Systematic, unintended drifts in the cyclic force produced with the fingertips

Satyajit Ambike[a], Daniela Mattos[b], Vladimir M. Zatsiorsky[c], Mark L. Latash[c]

[a] *Department of Health and Kinesiology, Purdue University, West Lafayette, IN*

[b]*Department of Psychological Sciences, University of Missouri, Columbia, MO*

[c]*Department of Kinesiology, The Pennsylvania State University, University Park, PA*

Keywords: cyclic action; isometric; finger force; referent configuration

Address for correspondence:

Satyajit Ambike
Department of Health and Kinesiology,
800 West Stadium Ave,
Purdue University,
West Lafayette, IN 47907
USA
Tel: (765) 496-0567
E-mail: sambike@purdue.edu

ABSTRACT

Cyclic isometric finger-force patterns established using visual feedback show systematic drifts when the feedback is removed. Force changes at multiple time scales and opposite directions have been reported. For further characterization of these drifts, healthy subjects produced isometric, cyclic finger force with and without visual feedback at various initial amplitudes and frequencies. We hypothesized that on feedback removal, the amplitude will be attracted towards a preferred value that is frequency dependent. We found that the amplitude always increased after feedback removal. The magnitude of amplitude change was proportional to initial frequency, but it was invariant over the explored range of initial amplitudes. Thus, the existence of a preferred amplitude of force oscillations was not supported. We interpret these results within the referent configuration and the referent configuration back-coupling hypotheses. These data will inform a mathematical model of finger-force drifts. However, currently they raise more questions than they answer, and a coherent account of finger-force drifts remains a challenge.

Introduction

Unintentional drifts in performance are rather common (e.g., Slifkin, Vaillancourt, & Newell, 2000; Vaillancourt & Russell 2000; Shapkova, Shapkova, Goodman, Zatsiorsky, & Latash, 2008; Heijnen, Muir, & Rietdyk, 2012; Heijnen, Romine, Stumpf, & Rietdyk, 2014; Zhou, Solnik, Wu, & Latash, 2014; Ambike, Zatsiorsky, & Latash, 2015; Ambike, Mattos, Zatsiorsky, & Latash, 2016). In particular, during accurate constant force production tasks in isometric conditions with visual feedback, turning the feedback off results in a slow consistent drift of the force, typically to lower magnitudes (Slifkin et al., 2000; Vaillancourt & Russell, 2002; Ambike et al., 2015). In normalized units (% maximum voluntary contraction), this drop in force is larger for the larger initial force magnitudes and can reach up to 30% of the initial force level over 20-30 s, without the subject being aware of the force drop (Ambike et al. 2015). This phenomenon has been interpreted as a reflection of a limitation of the working memory (Slifkin et al., 2000, Vaillancourt & Russell, 2002), supported by later studies of cortical activation using both EEG (Poon, Chin-Cottongim, Coombes, Corcos, & Vaillancourt, 2012) and MRI-based methods (Vaillancourt, Thulborn, & Corcos, 2003).

A conceptually different explanation has been suggested (Ambike et al., 2015; Jo, Ambike, Lewis, Huang, & Latash, 2015) based on a physical approach to human motor actions (reviewed in Latash, 2016). According to this approach, force production in isometric conditions is associated with setting a referent coordinate (RC) for the effector and a magnitude of apparent stiffness (*k*, which is a reflection of shifts in spatial RCs for the participating muscles) (Pilon, De Serres, & Feldman, 2007; Latash, 2010; Feldman, 2015; Ambike, Paclet, Zatsiorsky, &

Latash, 2014; Ambike, Mattos, Zatsiorsky, & Latash, 2016b). Force (F) emerges at the interface of the effector and the environment such that its magnitude is defined by the difference between the RC and the stationary actual coordinate (AC) of the effector, and the apparent stiffness: $F = k(RC – AC)$. The reported slow drop in force indicates that RC drifts toward AC and/or k drops. Note that k serves as a measurable surrogate variable that represents the influence of multiple muscles on the behavior of an end effector. As such, k can be modulated by altering the co-contraction of antagonist muscle pairs. A recent study has provided evidence for a drift of RC toward AC, while changes in k were inconsistent across subjects (Ambike, Mattos, Zatsiorsky, & Latash, 2017). Hence, here we consider the RC drift as the main mechanism of unintentional force change. If the system were able to reach the RC (AC = RC), the force would vanish, muscle activation would be minimal, and the system would be in an equilibrium state with minimum potential energy. Hence, motion of RC toward AC drives the system toward the state of minimum potential energy.

Brain imaging studies suggest that different neural substrates are involved in the control of cyclic and discrete movements (akin to the steady force-production tasks described above) (Schaal, Sternad, Osu, & Kawato, 2004; Yu, Sternad, Corcos, & Vaillancourt, 2007; Graziano, Taylor, & Moore, 2002). Sternad and Hogan (2007) developed the theoretical taxonomy to distinguish between the two kinds of movements. We followed this fundamental distinction between movement types and found unintentional changes in performance during tasks involving accurate cyclical force production in isometric conditions while the subject is paced by a metronome (Ambike et al., 2016). Typically, turning the visual feedback off leads to a relatively slow drop in the mean value of force (with the characteristic times of 10-20 s) accompanied by a quick increase in the peak-to-peak amplitude of the cyclical force changes (with the characteristic times of 1-2 s). These observations have led to a hypothesis that at least two mechanisms contribute to the unintentional force changes. The first is the aforementioned RC drift toward AC leading to the drop in the steady-state task component (mean force magnitude). The second is the drift of the cyclical force amplitude (A_F) to a preferred value ($A_{F\text{-}PREF}$). Note that preferred amplitudes of cyclical motor actions have been reported and explored earlier (Kay, Kelso, Saltzman, & Schoner, 1987; Hatsopoulos & Warren, 1996).

The primary purpose of this study was to explore the mechanism of force amplitude increase by varying the initial force amplitude (A_{TASK}) during cyclical force production. Indeed, if there is a drift toward $A_{F\text{-}PREF}$, increasing A_{TASK} could be expected to lead to smaller unintentional increase in A_F. If A_{TASK} is larger than $A_{F\text{-}PREF}$, an unintentional drop in A_F is expected. Earlier studies have shown that the unintentional drift in force magnitude during steady-state constant-force-production tasks was proportional to the initial force magnitude (Vaillancourt & Russell, 2002; Ambike et al., 2015). Based on this finding, one could have an expectation that the increase in A_F during the cyclical force production tasks observed after turning the visual feedback off would also increase proportionally to A_{TASK}. Our first specific working hypothesis (Hypothesis 1), in line with the first argument above, was that the relative increase in A_F, expressed as a percentage of A_{TASK}, would decrease with an increase in A_{TASK}, and it would become negative for a sufficiently high A_{TASK}. Since the two mechanisms of force changes, those leading to mean force (M_F) and A_F changes, are assumed to be independent, we expected that M_F would show a consistent drift to lower values (as in Ambike et al., 2016) without effects of A_{TASK} or oscillation frequency (see below) on the magnitude of that drift (Hypothesis 2).

We also explored possible effects of frequency of force production (f_{TASK}) on the characteristics of the two drift processes. Earlier studies have shown that increasing the frequency of a cyclic motor action can lead to a drop in the preferred amplitude of that action (Kay et al., 1987; Hatsopoulos & Warren, 1996; Bonnard & Pailhous, 1999). Hence, increasing f_{TASK} was expected to lead to a drop in $A_{F\text{-}PREF}$. As a result, we expected a smaller relative increase in A_F with an increase in f_{TASK} (Hypothesis 3). This exploration is intended to help in our plans to develop a mathematical model of the processes involved in unintentional force changes.

METHODS

Subjects

Fourteen adults participated in this study (6 males and 8 females; age: 29.36 ± 9.07 yr., height: 172.14 ± 8.87 cm, weight: 68.57 ± 14.50 kg; mean ± SD). The subjects were right-hand dominant by self-report and had no history of upper arm injury or discomfort for the past six months. All participants signed an informed consent form in compliance with the protocol approved by the Office for Research Protection of the Pennsylvania State University.

Equipment and procedures

Subjects sat in a chair with their right forearm resting on top of a table. Each subject was allowed to choose a comfortable hand posture with all fingers comfortably extended. The hand posture was consistent across trials. The subjects placed the fingertips on four force sensor (PCB model 208C01, PCB Piezotronics, Depew, NY) as shown in Fig. 1A. The diameter of the sensors was 17 mm. Sandpaper (100-grit) was placed on the contact surface of the sensor to increase the sensor-finger friction. The signals from the transducers were sent to a PCB 484B11 signal conditioner and digitized at 200 Hz using a 16-bit National Instruments PCI-6052E analog-to-digital card (National Instruments, Austin, TX). The sensor reading was zeroed with the subject’s fingers resting on the sensors and with the hand relaxed just before data collection so that only the active downward forces were measured by the sensors. A customized LabVIEW program was used for the data acquisition and for subject feedback. The sum of all four finger forces was provided as visual feedback using a 19-inch monitor placed at 0.8 m in front of the subject.

The experiment started with two maximal voluntary contraction (MVC) trials using four fingers. Subjects pressed as hard as possible on the sensors for 6 s. There was a 30-s rest between the two trials. Visual feedback of the produced force was provided. The highest MVC between the two trials was used to normalize the experimental task.

The experimental task consisted of producing cyclical changes in the total pressing force using the index, middle, ring, and little fingers simultaneously. Two horizontal lines on the monitor indicated the upper and lower force targets (Fig 1B). The subjects were paced by an auditory metronome at twice the required force frequency, so that subjects reached the targets at each beat. Each trial lasted 25 s and the visual feedback on the total force was removed after the first 10 s. Subjects were instructed to be as accurate as possible when the visual feedback was present, and to continue performing the task in absence of visual feedback, until a text message appeared indicating that the trial was finished. The visual feedback gain was manipulated so that the two horizontal target lines appeared at the same locations for all A_{TASK} conditions. This way, the visual feedback was identical across all conditions, even as the participant produced different force amplitudes across various trials.

< FIGURE 1 ABOUT HERE>

The mean force (M_{TASK}) was always 25% of the MVC. There were 4 levels of force amplitude (A_{TASK}): 5, 10, 15, and 20% of the MVC. Ambike et al., (2016) observed approximately a 50% increase in the amplitude after visual feedback had been removed when A_{TASK} = 10%. Therefore, it was expected that the relative change in amplitude would reduce as A_{TASK}

increased for the first three A_{TASK} values, and it could become negative for A_{TASK} = 20% (Hypothesis 1). There were 4 action frequencies (f_{TASK}): 0.5, 0.75, 1, 1.5 Hz, and the metronome was set at twice these values. Each condition was repeated three times. The combinations of A_{TASK} and f_{TASK} were randomly manipulated across trials. There were 30-s breaks after each trial, and longer breaks of at least 3 min after 16 trials or as needed.

Familiarization trials were performed at the beginning of the experiment. Practice was provided in two parts. In the first part, the participants performed the task with full visual feedback. A_{TASK} was fixed at 15% of the MVC, and the frequency progressed from the intermediate (0.75 and 1 Hz) to the boundary (0.5 and 1.5 Hz) values across the practice trials. Next, the task was practiced as it would be done during the experiment (with the visual feedback being turned off) with A_{TASK} of 5% MVC and at the two boundary frequency values. The participants never started the experiment with a condition that they had practiced immediately before. The training lasted for about 7 min.

Data analysis

MATLAB programs were written for data analysis. The vertical finger forces were filtered using a low-pass, zero-lag, fourth-order Butterworth filter with the cutoff frequency of 10 Hz. The filtered individual finger forces were summed up to obtain the total finger force. All total force trajectories were normalized by the corresponding MVC value, and further analysis was conducted on the normalized total forces.

<FIGURE 2 ABOUT HERE>

The oscillation phase at the 10-s mark (when the visual feedback was turned off) varied across trials. Therefore, the mean force and the force amplitude were computed for each oscillation cycle as the mean force value of the consecutive extrema, and the absolute difference between the consecutive extrema, respectively. These values were assigned to the middle of the time interval between the two extrema. The mean force and force amplitude values were pooled across trials and then binned along the time axis. Three bins were chosen to represent the *initial phase* of the oscillation (Phase 1) before the visual feedback was turned off (6 s to 10 s), the *middle phase* (Phase 2) two seconds after the feedback was turned off (12 s to 16 s), and the *final phase* of the oscillation (Phase 3) after the visual feedback was turned off (21 s to 25 s), see Figure 2. The amplitude change takes about 1 to 2 seconds to saturate (Ambike et al., 2016), and the timing of Phase 2 allows for this change to occur. The mean forces, M_F, and the mean oscillation amplitudes, A_F, within these time bins were computed. Statistical analysis was conducted on the changes in these quantities. We defined the change Δ*Phase 12* as the difference between the values of M_F (and A_F) in Phase 2 and Phase 1. Similarly, Δ*Phase 13* was defined as the difference in values between Phase 3 and Phase 1. Thus, the mean force change, ΔM was computed as ($M_{F\text{-middle}} – M_{F\text{-initial}}$) for Δ*Phase 12* and as ($M_{F\text{-final}} – M_{F\text{-initial}}$) for Δ*Phase 13*. Similarly, the amplitude change, ΔA was quantified as ($A_{F\text{-middle}} – A_{F\text{-initial}}$) for Δ*Phase 12* and as ($A_{F\text{-final}} – A_{F\text{-initial}}$) for Δ*Phase 13.* The percent amplitude change was computed as: $\%\Delta A = 100 \times \Delta A/A_{F\text{-initial}}$. Since the initial M_{TASK} was always the same across conditions, we did not perform a separate analysis of percent change in M_F.

Statistics

Most data are presented as means and standard errors (SE). To investigate the effects of instructed initial amplitude (A_{TASK}) and frequency (f_{TASK}) on the percent amplitude change (Hypotheses 1 and 3), $\%\Delta A$ was subjected to a 3-way, repeated-measures ANOVA with factors Δ*Phase* (levels: Δ*Phase 12 and* Δ*Phase 13*), Frequency f_{TASK} (4 levels), and Amplitude A_{TASK} (4 levels). A similar, independent analysis with the same factors and levels was performed for the change in mean force ΔM (Hypothesis 2). Finally, we also investigated the effect of the task parameters on the absolute change in the amplitude: ΔA was subjected to a 3-way, repeated measures ANOVA with the same factors and levels.

All statistics were performed using an α level of 0.05. Mauchly’s sphericity tests were performed to verify the validity of using repeated-measures ANOVA. The Greenhouse–Geisser adjustment to the degrees of freedom was applied whenever departure from sphericity was observed. Significant effects of ANOVA were further explored using pairwise comparisons with Bonferroni corrections. All statistics were performed with SPSS statistical software.

RESULTS

Typical subject response

Subjects showed consistent changes in the two characteristics of the cyclical force patterns, peak-to-peak amplitude (A_F) and mean value (M_F). Figure 2 depicts the typical response in a single trial. After the removal of visual feedback, typically, M_F reduced and A_F increased. Both changes started simultaneously, but proceeded at significantly different time scales. In particular, A_F showed no consistent changes after the initial quick increase, while M_F showed a slow, consistent drift to lower values.

Figures 3 and 4 depict the across-subject mean values of M_F and A_F for different combinations of A_{TASK} and f_{TASK}, respectively. The force means and amplitudes from all trials of all subjects are pooled into 1-second bins for these plots. We decided not to plot error bars in these figures because they make the plots unreadable. We fit exponential functions of the form $y = a \times e^{(-t/\tau)} + b$, consistent with previous work (Ambike et al., 2015, Ambike et al., 2016), to the across-subject averages of the mean and amplitude independently for each f_{TASK} and A_{TASK} condition, i.e., to each curve depicted in Figures 3 and 4. M_F dropped exponentially after the feedback removal (median and inter-quartile range for the R^2 across the exponential fits for all f_{TASK} and A_{TASK} were 0.98 and 0.01, respectively), and the time constant τ, averaged across all data, was 9.79 ± 0.8 s. Similarly, A_F showed an exponential increase (median and inter-quartile range for the R^2 across the exponential fits for all f_{TASK} and A_{TASK} conditions were 0.91 and 0.1, respectively). The overall time constant τ for this increase was 1.29 ± 0.1 s.

<FIGURE 3 ABOUT HERE>

<FIGURE 4 ABOUT HERE>

Changes in mean force and force amplitude

Recall that we expected the percent change in amplitude (%ΔA) to reduce with both A_{TASK} and f_{TASK} (Hypotheses 1 and 3, respectively). The ANOVA revealed a main effect of A_{TASK} on %ΔA [$F_{(1.941, 25.230)} = 47.511$; $p < 0.01$]. Mean ± SE for %ΔA are 113.37 ± 13.96%, 90.89 ± 15.86%, 59.52 ± 12.83%, and 40.91 ± 10.92%, for the four A_{TASK} conditions (in increasing order of A_{TASK}). Pair-wise comparisons revealed significant differences in all but the first two A_{TASK} conditions, indicating that %ΔA decreased as A_{TASK} increased – see Figure 5. There was also a significant effect of %ΔA f_{TASK} on %ΔA [$F_{(1.911, 24.848)} = 6.302$; $p < 0.01$]. Pair-wise comparisons revealed one pair with a significant difference: 0.5 Hz (87.22 ± 15.52%) > 1.5 Hz (66.368 ± 11.59%), suggesting that %ΔA reduced as f_{TASK} increased.

<FIGURE 5 ABOUT HERE>

There was no effect of Δ*Phase* ($p = 0.119$; $F_{(1,13)} = 2.79$), reflecting the fact that amplitude changes saturated rather quickly (see Figures 3 and 4). Finally, there was a significant Δ*Phase* x A_{TASK} interaction [$F_{(2.108, 27.410)} = 16.892$; $p < 0.01$] reflecting the following observation: for the smallest A_{TASK}, %ΔA for Δ*Phase 13* was larger than that for Δ*Phase 12*. However, this difference across Δ*Phase* reduced with higher A_{TASK}s, and it reversed for the largest A_{TASK}.

The mean force was expected to drop after visual feedback removal, without an effect of A_{TASK} and f_{TASK} (Hypothesis 2). The grand mean for ΔM was -0.048 ± 0.009 NFU (95% confidence interval: [-0.067, -0.028]), indicating that the force consistently reduced after visual feedback removal – see Figure 6. Furthermore, we found that mean force drop approximately doubled over the 15 s of task performance with no visual feedback [$\Delta M(\Delta \mathit{Phase}\ 12) = -0.033 \pm 0.008$ NFU; $\Delta M(\Delta \mathit{Phase}\ 13) = -0.062 \pm 0.01$ NFU], indicating that the force drop occurred over the entire duration of the no-feedback portion of the trial (Main effect of Δ*Phase*: $F_{(1,13)} = 77.604$; $p < 0.01$). The mean force drop also showed a modest tendency to increase with f_{TASK} [$F_{(3,39)} = 5.494$; $p < 0.01$]. $\Delta M = -0.043 \pm 0.01$ NFU, -0.044 ± 0.01 NFU, -0.052 ± 0.009 NFU, and -0.052 ± 0.009 NFU for the 0.5 Hz, 0.75 Hz, 1 Hz and the 1.5 Hz oscillation frequencies, respectively. However, pair-wise comparisons revealed no significantly different pairs. Finally, there was no effect of A_{TASK} on the amount of force drop ($p = 0.126$).

<FIGURE 6 ABOUT HERE>

The changes in %ΔA could occur due to changes in A_{TASK}, ΔA or both. To understand the cause of the change in the relative amplitude increase, we explored the absolute change in the oscillation amplitude. The grand mean of ΔA was 0.091 ± 0.01 NFU (95% confidence interval: [0.054, 0.129]), which implies that the amplitude always increased – see Figure 7. Furthermore, there was no main effect of A_{TASK} on ΔA ($p = 0.148$). Since $\%\Delta A = 100 \times \Delta A / A_{\mathrm{F\text{-}initial}}$, and $A_{\mathrm{F\text{-}initial}}$ is mostly determined by A_{TASK}, this result suggests that the reduction in %ΔA with A_{TASK} was mostly due to the increased A_{TASK}. Consistent with the ANOVA results for %ΔA, ΔA revealed no effect of Δ*Phase* ($p = 0.266$), and a significant effect of f_{TASK} ($F_{(3,39)} = 4.105$; $p < 0.05$). The mean values for ΔA were 0.102 ± 0.02 NFU, 0.092 ± 0.01 NFU, 0.089 ± 0.01 NFU, and 0.083 ± 0.01 NFU for the 0.5 Hz, 0.75 Hz, 1 Hz and the 1.5 Hz frequency oscillations, respectively. But pair-wise comparisons did not reveal any significantly differing pairs, suggesting a tendency for ΔA to decrease with f_{TASK}. Finally, there was a Δ*Phase* x A_{TASK} interaction ($F_{(3,39)} = 10.078$; $p < 0.01$) reflecting the fact that ΔA showed an increase from Δ*Phase 12* to Δ*Phase 13* for $f_{\mathrm{TASK}} = 0.5$ Hz, but this increase vanished as f_{TASK} increased, and reversed for the 1.5 Hz oscillation frequency.

<FIGURE 7 ABOUT HERE>

DISCUSSION

The general pattern of our results is consistent with earlier publications on force changes after visual feedback removal (Slifkin et al., 2000; Vaillancourt & Russell, 2002; Ambike et al., 2015, Ambike et al., 2016). In particular, the mean force dropped with characteristic times of about 10 s, while the amplitude increased much faster, with characteristic times of 1-2 s.

Most of our specific hypotheses formulated in the Introduction were validated by our data. First, we expected the percent change in the amplitude to reduce as A_{TASK} increased, and finally reverse for the highest A_{TASK} (Hypothesis 1). This hypothesis has been confirmed, but only in part. Indeed, the percent amplitude change $\%\Delta A$ reduced with A_{TASK}, but it did not become negative within the studied range of A_{TASK}. In fact, analysis of the absolute change in amplitude ΔA revealed that the amplitude always increased by roughly the same absolute amount regardless of A_{TASK}. We found that the mean force decreased with time, and this was affected by oscillation frequency (Hypothesis 2). Finally, the amplitude change decreased as oscillation frequency increased (Hypothesis 3).

Two observations from this study are particularly striking: (1) the almost constant magnitude of the increase in oscillation amplitude for a range of A_{TASK}, and (2) the counter-directional changes in M_F and A_F when visual feedback is removed. These observations have implications on such topics as the control of action with referent coordinates (RCs), and the character and causes of unintentional drifts in RCs. We discuss these ideas below, but acknowledge that our results raise more questions than they answer.

Control of action with shifts in referent coordinates

Our view of the mechanisms underlying human motor action is based on the physically and physiologically grounded idea of equilibrium point (EP) control (Feldman, 1966). The EP hypothesis pertains to the action of a single muscle, and it was generalized to multi-muscle systems as the referent configuration hypothesis (Feldman, 2009, 2015). Within this view, at any level of the control hierarchy, the input defines referent coordinates (RCs) for salient effectors such as muscles, joints, limbs, and the whole body. A series of few-to-many (redundant) mappings converts task-specific RCs to RCs at lower level, down to the thresholds of the tonic stretch reflexes (λ), which represent RCs at the muscle level (for more detail, see Latash, 2010). The peripheral consequences of setting the RCs depend on the constraints imposed by the environment. In particular, in isometric conditions, a force at the body-environment interface emerges.

In the case of isometric fingertip force production task studied in this paper, the central controller is assumed to specify a RC for the fingertip, which is below its current actual coordinate (AC). The sensor surface constrains the position of the fingertip, and a force at the fingertip-sensor interface emerges (Latash, 2010; Feldman, 2015; Ambike et al., 2014, Ambike et al., 2016b). We assume that the cyclic task of this study was associated with setting a cyclically oscillating fingertip RC. Since the AC is static (except for small changes due to fingertip deformations – ignored in this study), the oscillating RC generates the oscillating fingertip force. Furthermore, the change in mean force is due to a drift in the mean value of the RC(t) trajectory towards the AC (documented in Ambike et al., 2016b), and the increase in the force amplitude is caused by a similar change in the RC(t) peak-to-peak amplitude.

Overall, we view the observed unintentional changes in force characteristics as reflections of the natural behavior of a physical system involving interactions between the body and environment (cf. Kugler & Turvey, 1987; Kelso, 1995), rather than computational processes within the central nervous system. The striking effects of turning the visual feedback off emphasize the importance of this sensory modality for accurate performance. Without this feedback, the system shows relaxation processes toward different (preferred) force characteristics despite the availability of unchanged somatosensory signals.

Unintentional drifts in referent coordinates – two processes

The two distinct time constants of the changes in mean and amplitude of the force suggest the presence of two separate physiological processes. The first process is the drift of the mean RC towards the AC. This process is consistent with the system trying to attain a state of minimal energy. The concept of *RC-back-coupling* (Wilhelm, Zatsiorsky, & Latash, 2013; Zhou et al., 2014; Ambike et al, 2015) has been suggested to account for such unintentional drifts in RCs. The changes in RC that drive changes in muscle activations and result in AC motion may be addressed as *direct coupling* (RC acting as an attractor for AC). These processes act at relatively short time delays that are typical of neural conduction and electromechanical delays (on the order of 0.1 s). In contrast, the hypothesized RC-back-coupling phenomenon (Wilhelm et al., 2013; Ambike et al., 2014, Ambike et al., 2015) drives the RC towards the AC when the AC cannot move. The RC back-coupling process seems to function over longer time scales (between 5 and 15 s) (Ambike et al., 2015 and our current data). Such unintentional actions have also been observed in limb positional tasks (Zhou et al., 2014) and prehension tasks

(Ambike et al., 2014). Recently, changes in RCs during the drift in isometric fingertip forces produced without visual feedback have been documented (Ambike et al., 2017).

The second process is the quick increase in amplitude. This cannot be interpreted as the system trying to reach a state of minimal energy. Based on our earlier work (Ambike et al., 2016), we hypothesized the presence of a limit cycle towards which the force profile drifted when visual feedback was removed. Note that limit-cycle dynamics have been observed in rhythmic manual behavior (Kay et al. 1987; Kelso, Holt, Rubin, & Kugler, 1981). A convergence towards a unique oscillation amplitude $A_{F\text{-}PREF}$ for a range of initial amplitudes would have confirmed the presence of a limit cycle. Our data do not support this hypothesis. Although the patterns of the force amplitude changes appear to confirm a drift towards a preferred force amplitude ($A_{F\text{-}PREF}$), there are two caveats. First, the amplitude change never became negative, indicating that our instructed amplitudes (A_{TASK}) was never greater than this hypothesized $A_{F\text{-}PREF}$. Second, the absolute A_F change was roughly equal for all the A_{TASK} values. We acknowledge that this later observation may be due to insufficient power of the study or the limited range of the explored A_{TASK}. However, the effect was far from significant, and we saw no visible trends in the data (Figure 7). Thus, we are unable to validate the existence of $A_{F\text{-}PREF}$, and are left with a rather unusual observation of constant ΔA for a range of A_{TASK}. Developing a mathematical model able to account for such behaviors is a challenge for our future work.

The existence of two drift processes at different characteristic times, 5-15 s for steady-state task components and 1-2 s for task with quick changes in the salient variable (Zhou et al., 2014; Ambike et al., 2015, 2016; Reschechtko, Zatsiorsky, & Latash, 2015), suggests that these processes originate in subspaces characterized by different relaxation times. Since any voluntary action involves multiple elements (e.g., multiple muscles involved in single-finger force production), it may be viewed as a superposition of two processes: Changes within the uncontrolled manifold (UCM, Scholz & Schoner, 1999) for the salient performance variable and orthogonal to the UCM (ORT). Lower stability within the UCM (Schoner 1995; Latash, Scholz & Schoner, 2007) corresponds to longer relaxation times, while higher stability along ORT corresponds to shorter relaxation times. It is possible, therefore, that the two different times of force change reflect processes within the UCM and ORT sub-spaces. Since both processes lead to changes in force, i.e., drifts along ORT, this hypothesis implies coupling between the UCM and ORT. So far, no experimental validation of such coupling has been reported; this remains a problem to be solved in future experiments.

Vaillancourt and colleagues (Slifkin et al., 2000; Vaillancourt & Russell, 2002) suggested that the force changes after visual feedback removal resulted from limited capacity of working memory. This notion, which we call ‘the memory hypothesis’, does not explain the observed unintentional actions, in particular the counter-directional changes in the mean and amplitude force characteristics. On the other hand, memory-like processes were observed for cyclical, isometric force production (Ambike et al., 2016). In particular, when participants interrupted cyclical force production with a rest interval, force changes consistent with those in continuous force production without feedback were observed on task resumption, suggesting that memory was, at least in part, responsible for the changes. Therefore, memory related processes may play a role in unintentional motor actions, but there are other processes that remain to be uncovered. The memory hypothesis is compatible with the idea of RC-back-coupling that may be viewed as a limited capacity to hold a prescribed RC in short-term motor memory.

Final Comments

The main limitation of this study is that the participants could only press on the sensors, and could not exert upward forces. This placed a lower bound on the generated force, and consequently limited the force amplitude that could be achieved. Additionally, the magnitude of the mean force itself was constrained by fatigue considerations. Our results (especially the approximate independence of force amplitude change of the instructed force amplitude) may be a consequence of these extraneous factors. The preferred amplitude $A_{F\text{-}PREF}$ might require a change in the force direction and/or exploration of a much wider range of force amplitudes.

Furthermore, we assumed that the changes in the force trajectories stemmed from a corresponding change in the fingertip RC. It is plausible that the fingertip apparent stiffness was also responsible for the observed changes. This hypothesis can be quantified using perturbation experiments. For example, the force response obtained by perturbing the fingertip position during an isometric force-production task can be used to deduce its referent coordinate (RC) and the apparent fingertip stiffness (*k*). This pair {RC; *k*}, measured at the effector level, serves as a surrogate for the neural control signals. This method has been implemented for arm motion, grip force modulation and isometric fingertip force production (Latash & Gottlieb, 1991; Latash, Aruin, & Zatsiorsky, 1999; Ambike et al., 2016), and recently, we measured the changes in fingertip {RC; *k*} values associated with the drop in force after visual feedback removal (Ambike et al., 2017). The apparent stiffness changes were present, but they were inconsistent across subjects. In contrast, RC always approached AC with time. Therefore, although it is plausible that force profiles in the present study changed due to changes in both R and *k*, we have assumed here that the effects of *k* changes were relatively modest. Obtaining {RC; *k*} trajectories for cyclic force-production remains a challenge.

Another criticism of this study is that the task we study is not ecologically valid per se. However, it is part of many valid prehensile tasks. Moreover, this study builds on previous work that investigates isometric finger pressing tasks (see Introduction). It is likely that the drifts in performance observed here may be influenced by their functional relevance during ecological tasks. We intend to explore this in the future.

Finally, we required the subjects ‘to execute the same action’ after visual feedback was removed. Our data shows that subjects failed to follow this instruction, even though they believed that they were ‘doing the same’, and even though the observed force changes were quite consistent. Maybe, subjects tried to keep the perceptual effects of force changes constant when feedback was removed (cf. Powers, 1973; Mansell, 2011). Then, adaptation of quickly-adapting pressure-sensitive receptors in the fingertips (Meissner and Pacinian corpuscle end-organs; Johansson & Flanagan, 2009) might lead to an increase in A_F. However, these remain pure conjectures.

ACKNOWLEDGEMENTS

The study was in part supported by NIH Grants NS-035032 and AR-048563.

REFERENCES

Ambike, S., Paclet, F., Zatsiorsky, V.M., Latash, M.L. (2014). Factors affecting grip force: anatomy, mechanics, and referent configurations. *Experimental Brain Research,* 232, 1219–1231.

Ambike, S., Zatsiorsky, V.M., Latash, M.L. (2015). Processes underlying unintentional finger-force changes in the absence of visual feedback. *Experimental Brain Research,* 233, 711-721.

Ambike, S., Mattos, D., Zatsiorsky, V.M., Latash, M.L. (2016). The nature of constant and cyclic force production: unintentional force-drift characteristics. *Experimental Brain Research,* 234, 197-208.

Ambike, S., Mattos, D., Zatsiorsky, V.M., Latash, M.L. (2016b). Synergies in the space of control variables within the equilibrium point hypothesis. *Neuroscience*, 315, 150-161.

Ambike, S., Mattos, D., Zatsiorsky, V.M., Latash, M.L. (2016). Unsteady steady states: Central causes of unintentional force drift. *Experimental Brain Research,* 234, 3597-3611.

Bonnard, M., & Pailhous, J. (1999). Contribution of proprioceptive information to preferred versus constrained space-time behavior in rhythmical movements. *Experimental Brain Research*, 128, 568-572.

Feldman, A.G. (1966). Functional tuning of the nervous system with control of movement or maintenance of a steady posture. II. Controllable parameters of the muscle. *Biophysics,* 11, 565–578.

Feldman, A.G. (2009). Origin and advances of the equilibrium-point hypothesis. *Advances in Experimental Medicine and Biology*, 629,637–643.

Feldman, A.G. (2015). *Referent control of action and perception: Challenging conventional theories in behavioral science*. Springer: NY.

Graziano, M.S.A., Taylor, C.S.R., Moore, T. (2002) Complex movements evoked by microstimulation of precentral cortex. *Neuron* 34, 841–851.

Hatsopoulos, N.G., & Warren, W.H. Jr (1996). Resonance tuning in rhythmic arm movements. *Journal of Motor Behavior*, 28, 3-14.

Heijnen, M.J., Romine, N.L., Stumpf, D.M., Rietdyk, S. (2014). Memory-guided obstacle crossing: more failures were observed for the trail limb versus lead limb. *Experimental Brain Research*, 232, 2131-2142.

Heijnen, M.J., Muir, B.C., Rietdyk, S. (2012). Factors leading to obstacle contact during adaptive locomotion. *Experimental Brain Research*, 223:219-231.

Jo, H.J., Ambike, S., Lewis, M.M., Huang, X., Latash, M.L. (2015). Finger force changes in the absence of visual feedback in patients with Parkinson’s disease. *Clinical Neurophysiology*, 127, 684-692.

Johansson, R.S., & Flanagan, J.R. (2009). Coding and use of tactile signals from the fingertips in object manipulation tasks. *Nature Reviews, Neuroscience*, 10, 345-359.

Kay, B.A., Kelso, J.A., Saltzman, E.L., Schoner, G. (1987). Space-time behavior of single and bimanual rhythmical movements: data and limit cycle model. *Journal of Experimental Psychology: Human Perception and Performance,* 13, 178-192.

Kelso, J.A.S. (1995). *Dynamic patterns: The self-organization of brain and behavior*. Cambridge: MIT Press.

Kelso, J.A.S., Holt, K.G., Rubin, P., Kugler, P.N. (1981). Patterns of human interlimb coordination emerge from the properties of non-linear limit cycle oscillatory processes. Theory and data. *Journal of Motor Behavior,* 13, 226-261.

Kugler, P.N. & Turvey, M.T. (1987). *Information, Natural law and self-assembly of rhythmic movement*. Hillsdale, NJ: Lawrence Erlbaum.

Latash, M.L., Gottlieb, G.L. (1991). Reconstruction of shifting elbow joint compliant characteristics during fast and slow movements. *Neuroscience*, 43, 697–712.

Latash, M.L., Aruin, A.S., Zatsiorsky, V.M. (1999). The basis of a simple synergy: Reconstruction of joint equilibrium trajectories during unrestrained arm movements. *Human Movement Science*, 18, 3–30.

Latash, M.L., Scholz, J.P., Schoner, G. (2007) Toward a new theory of motor synergies. *Motor Control*, 11, 276-308.

Latash, M.L. (2010). Motor synergies and the equilibrium-point hypothesis. *Motor Control*, 14, 294-322.

Latash, M.L. (2016). Towards physics of neural processes and behavior. *Neuroscience and Biobehavioral Reviews*, 69, 136-146.

Mansell, W. (2011). Control of perception should be operationalized as a fundamental property of the nervous system. *Topics in Cognitive Science*, 3, 257-261.

Pilon, J-F, De Serres, S.J., Feldman, A.G. (2007). Threshold position control of arm movement with anticipatory increase in grip force. *Experimental Brain Research*, 181, 49-67.

Poon, C., Chin-Cottongim, L.G., Coombes, S.A., Corcos, D.M., Vaillancourt, D.E. (2012). Spatiotemporal dynamics of brain activity during the transition from visually guided to memory-guided force control. *Journal of Neurophysiology,* 108, 1335-1348.

Powers, W.T. (1973). *Behavior: The control of perception*. Chicago: Aldine.

Reschechtko, S., Zatsiorsky, V.M., Latash, M.L. (2015). Task-specific stability of multifinger steady-state action. *Journal of Motor Behavior*, 47, 365-377.Sanes, J.N., Mauritz, K-H, Evarts, E.V., Dalakas, M.C., Chu, A. (1984). Motor deficits in patients with large-fiber sensory neuropathy. *Proceedings of the National Academy of Science* 81, 979-982.

Sanes, J.N., Mauritz, K-H, Evarts, E.V., Dalakas, M.C., Chu, A. (1984). Motor deficits in patients with large-fiber sensory neuropathy. *Proceedings of the National Academy of Science* 81, 979-982.

Schaal, S., Sternad, D., Osu, R., Kawato, M. (2004) Rhythmic arm movement is not discrete. *Nature Neuroscience* 7, 1136–1143.

Scholz, J.P., Schoner, G. (1999). The uncontrolled manifold concept: identifying control variables for a functional task. *Experimental Brain Research*, 126, 289-306.

Schoner, G. (1995). Recent developments and problems in human movement science and their conceptual implications. *Ecological Psychology,* 8, 291-314.

Shapkova, E.Y., Shapkova, A.L., Goodman, S.R., Zatsiorsky, V.M., Latash, M.L. (2008). Do synergies decrease force variability? A study of single-finger and multi-finger force production. *Experimental Brain Research*, 188, 411–425.

Slifkin, A.B., Vaillancourt, D.E., Newell, K.M. (2000). Intermittency in the control of continuous force production. *Journal of Neurophysiology,* 84, 1708–1718.

Sternad, D., Hogan, N. (2007) On rhythmic and discrete movements: reflections, definitions and implications for motor control. *Experimental Brain Research*, 181, 13-30.

Vaillancourt, D.E., Russell, D.M. (2002). Temporal capacity of short-term visuomotor memory in continuous force production. *Experimental Brain Research*, 145:275-285.

Vaillancourt, D.E., Thulborn, K.R., Corcos, D.M. (2003). Neural basis for the processes that underlie visually guided and internally guided force control in humans. *Journal of Neurophysiology,* 90, 3330-3340.

Wilhelm, L., Zatsiorsky, V.M., Latash, M.L. (2013). Equifinality and its violations in a redundant system: multifinger accurate force production. *Journal of Neurophysiology*, 110, 1965-1973.

Zhou, T., Solnik, S., Wu, Y.S., Latash, M.L. (2014). Unintentional movements produced by back-coupling between actual and referent body configurations: violations of equifinality in multi-joint positional tasks. *Experimental Brain Research*, 232:3847-3859

Yu, H., Sternad, D., Corcos, D.M., Vaillancourt, D.E. (2007) Role of hyperactive cerebellum and motor cortex in Parkinson's Disease. *NeuroImage* 35, 222–233.

FIGURES

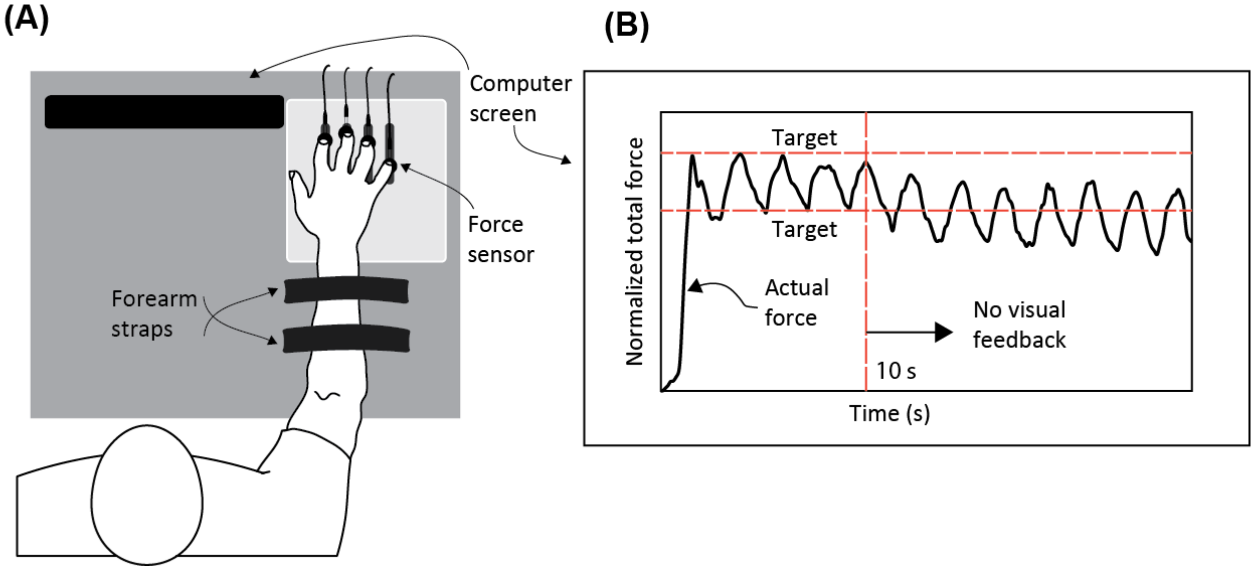

Figure 1. (A) Experimental setup. (B) Visual feedback of the force provided to the subject on a computer screen. Two horizontal lines indicated the instructed maximum and minimum of the force. The subject’s total finger force was provided for the first 10 s of the task and then removed.

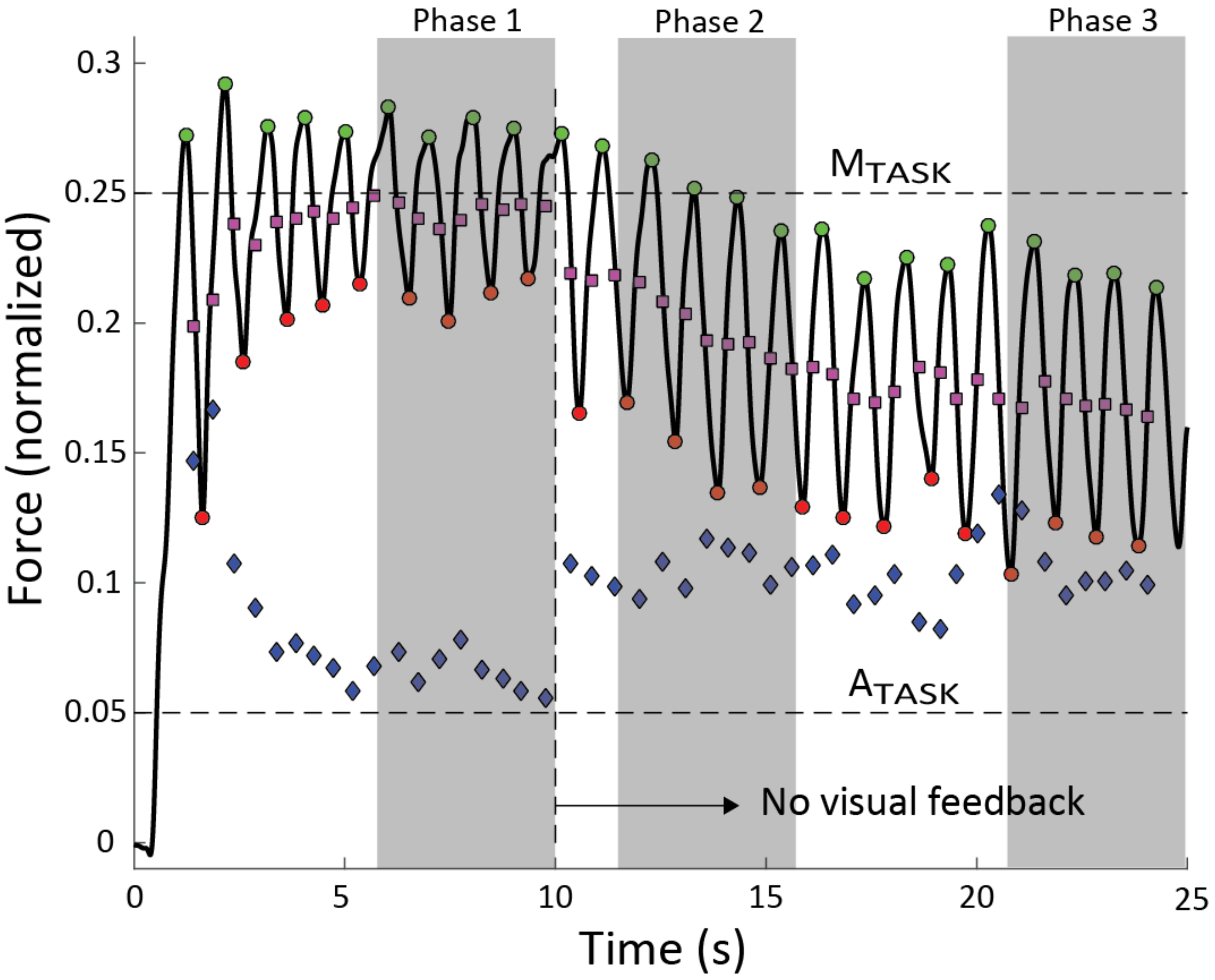

Figure 2. Typical subject response. The oscillation is established with visual feedback in the first 10 s of the trial. The feedback is removed at the 10th second, following which the mean and the amplitude of the oscillation change. The solid curve is the force-time trajectory. The circular marks on the trajectory locate the extrema. The square markers indicate the mean force and the diamond-shaped markers indicate the amplitude of oscillation. The three phases for pooling data for the subsequent statistical analysis are shown as shaded rectangles.

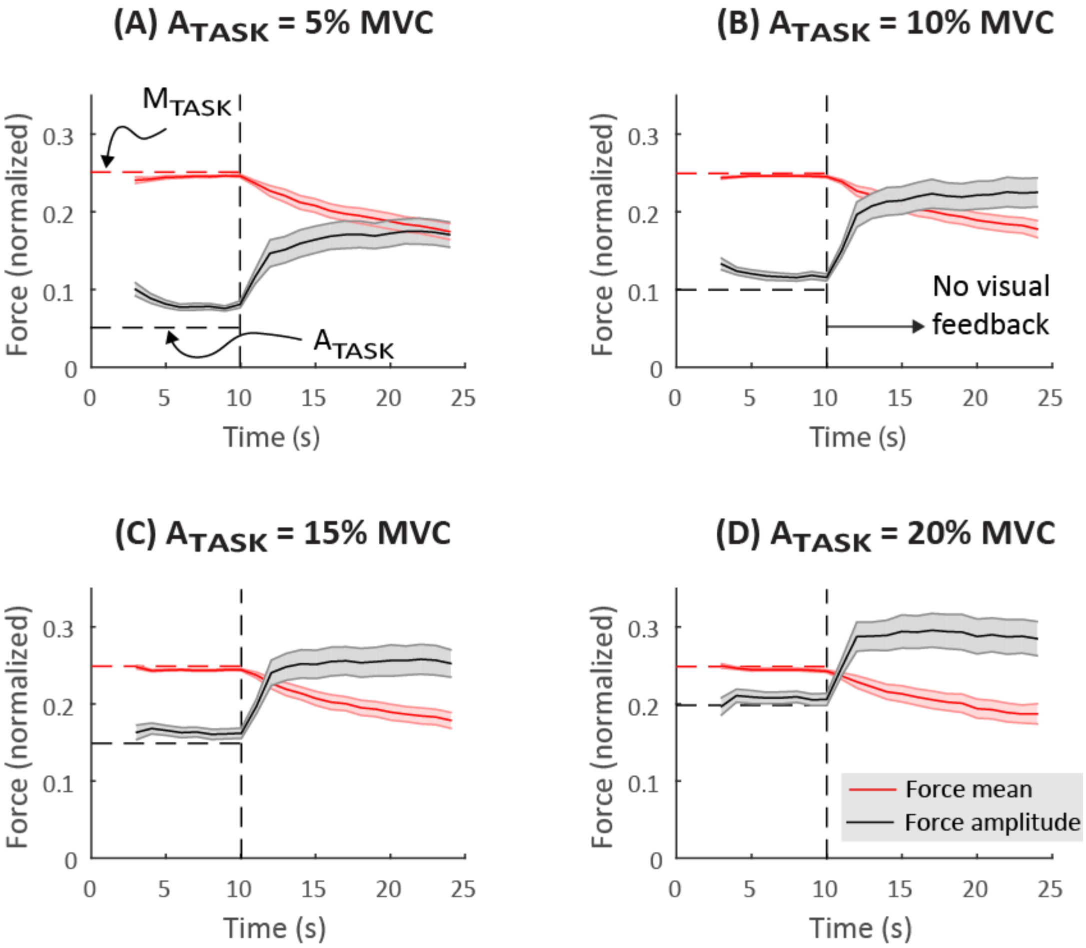

Figure 3. Across-subject and across-frequency average changes in the force means and amplitudes, grouped according to A_{TASK}. The feedback is removed at the 10th second. After that instant, curves for the mean force drop, and the curves for the amplitudes rise across conditions.

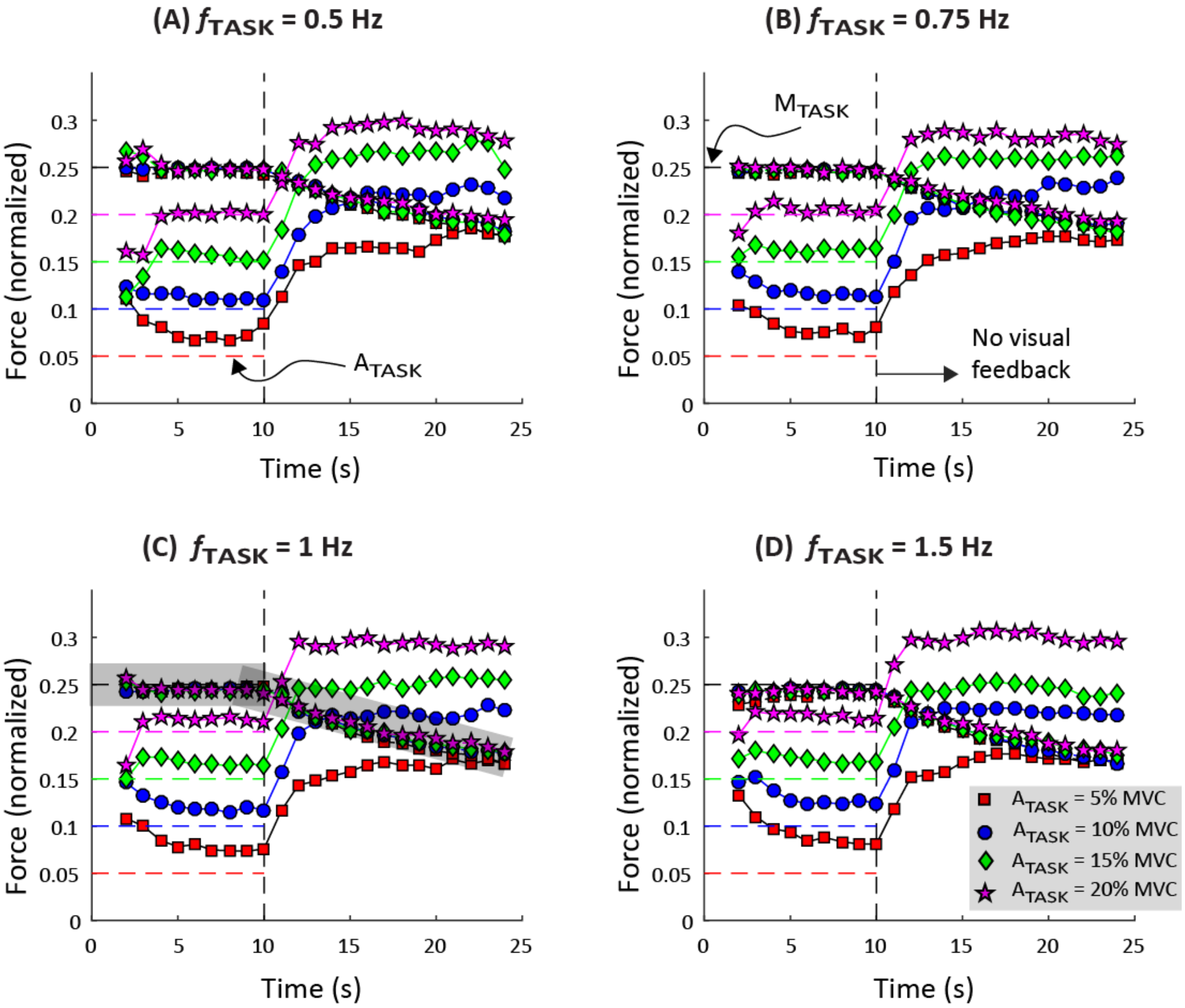

Figure 4. Across-subject average changes in the force means and amplitudes, grouped according to f_{TASK}. SE bars are omitted for clarity. The feedback is removed at the 10th second. After that instant, curves for the mean force drop, and the curves for the amplitudes rise across conditions. The curves for the mean force are highlighted in Panel (C) in the shaded areas.

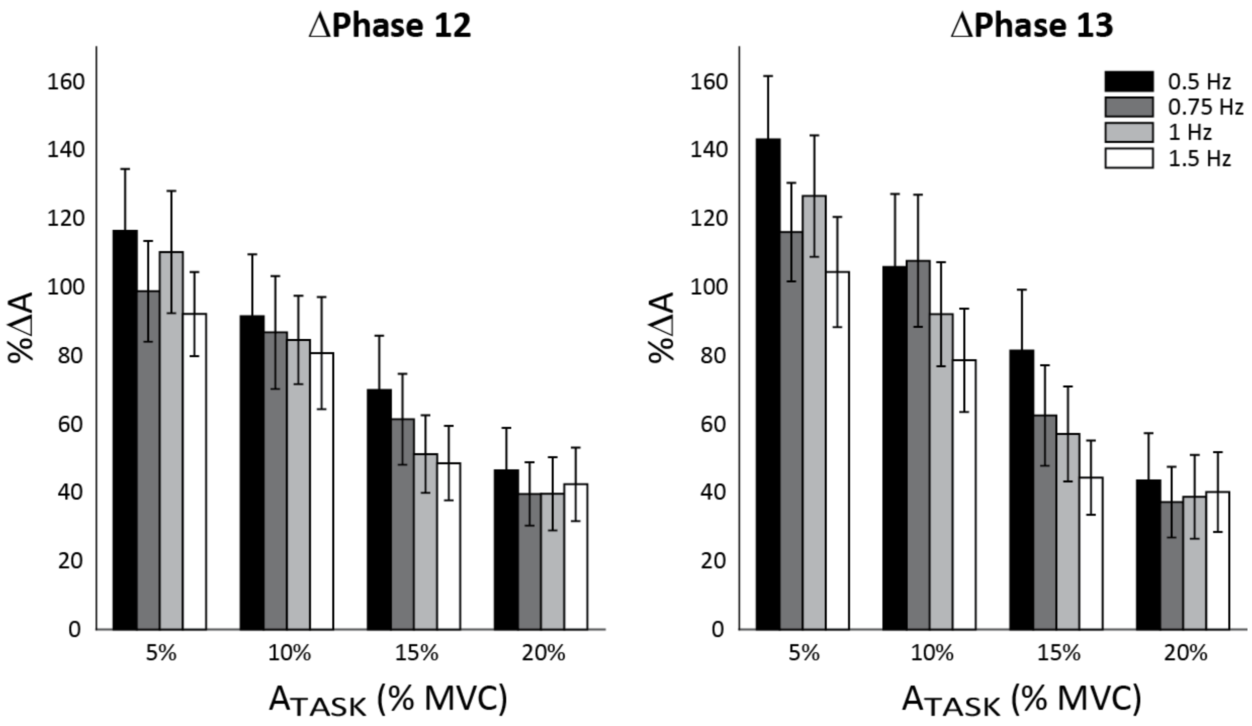

Figure 5. Mean ± SE of %∆A plotted across ∆*Phase*, A_{TASK} and f_{TASK}. A_{TASK} and f_{TASK} are the oscillation parameters established with visual feedback. %∆A is the relative change in amplitude after feedback removal. ∆*Phase* 12 and ∆*Phase* 13 represent the change in the parameter between Phases 1 and 2 and Phases 1 and 3, respectively, as indicated in Figure 2.

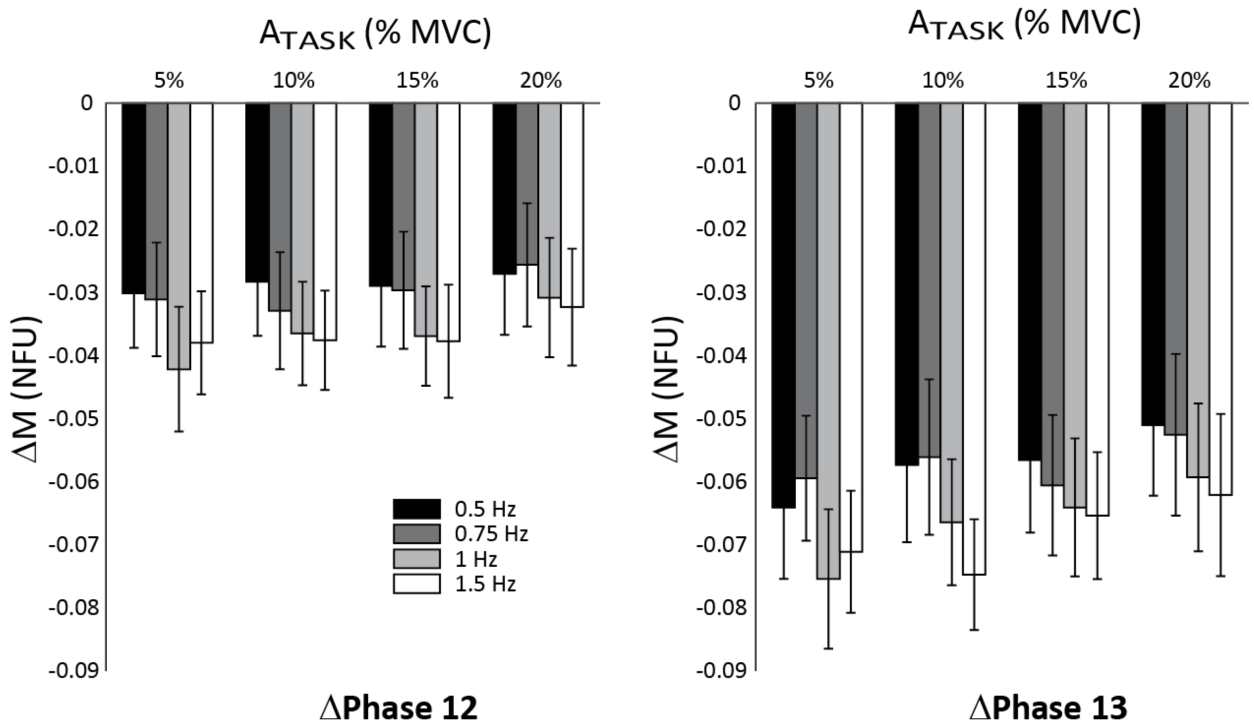

Figure 6. Mean ± SE of ΔM plotted across Δ*Phase*, A_{TASK} and f_{TASK}. A_{TASK} and f_{TASK} are the oscillation parameters established with visual feedback. ΔM is the change in the mean force after feedback removal. Δ*Phase* 12 and Δ*Phase* 13 represent the change in the parameter between Phases 1 and 2 and Phases 1 and 3, respectively, as indicated in Figure 2.

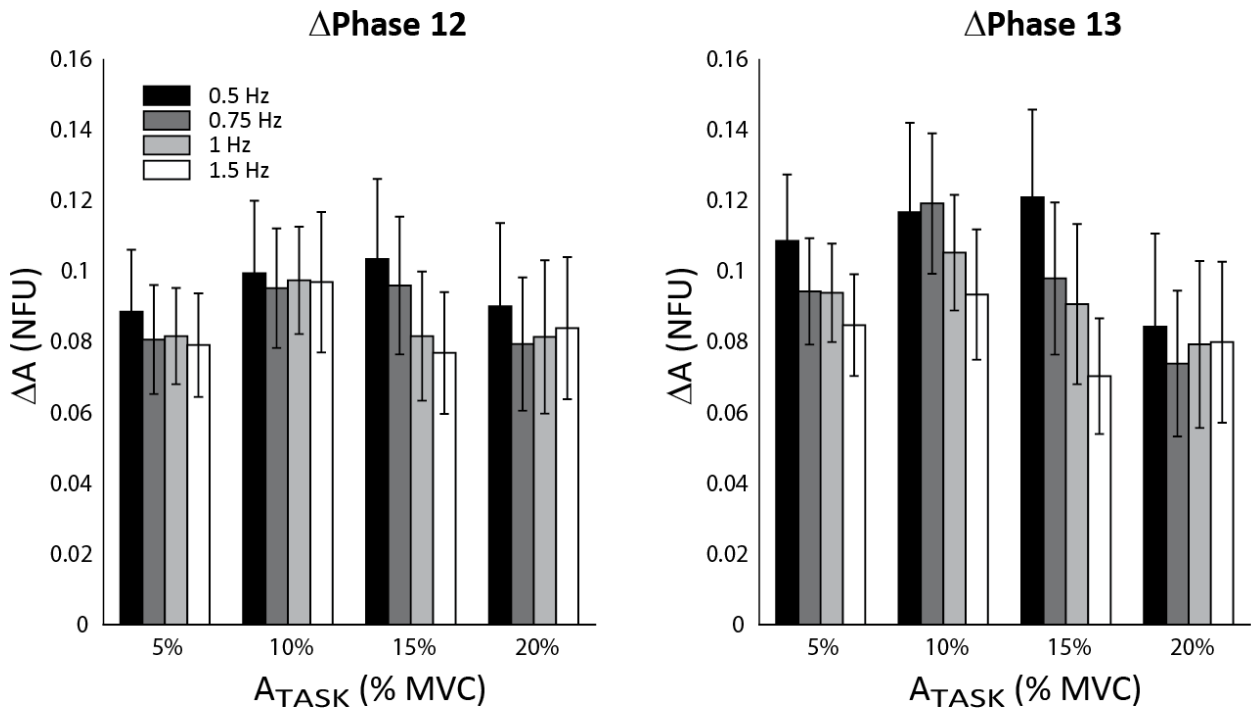

Figure 7. Mean ± SE of ΔA plotted across Δ*Phase*, A_{TASK} and f_{TASK}. A_{TASK} and f_{TASK} are the oscillation parameters established with visual feedback. ΔA is the absolute change in amplitude after feedback removal. Δ*Phase* 12 and Δ*Phase* 13 represent the change in the parameter between Phases 1 and 2 and Phases 1 and 3, respectively, as indicated in Figure 2.